Physica A 390 (2011) 2435–2441

Contents lists available at ScienceDirect

Physica A

journal homepage: www.elsevier.com/locate/physa

Fisher information description of the classical–quantal transition

A.M. Kowalski [a,d], M.T. Martín [a,e], A. Plastino [a,e], O.A. Rosso [b,c,e,*]

[a] Instituto de Física, Facultad de Ciencias Exactas, Universidad Nacional de La Plata (UNLP), C.C. 727, 1900 La Plata, Argentina

[b] Departamento de Física, Instituto de Ciências Exatas, Universidade Federal de Minas Gerais, Av. Antônio Carlos, 6627 - Campus Pampulha, 31270-901 Belo Horizonte - MG, Brazil

[c] Chaos & Biology Group, Instituto de Cálculo, Facultad de Ciencias Exactas y Naturales, Universidad de Buenos Aires, Pabellón II, Ciudad Universitaria, 1428 Ciudad Autónoma de Buenos Aires, Argentina

[d] Comisión de Investigaciones Científicas (CICPBA), Argentina

[e] Consejo Nacional de Investigaciones Científicas y Técnicas (CONICET), Argentina

ARTICLE INFO

Article history:
Received 5 December 2010
Received in revised form 2 February 2011
Available online 1 March 2011

Keywords:
Information theory
Fisher information
Statistical complexity
Semiclassical theories
Quantum chaos

ABSTRACT

We investigate the classical limit of the dynamics of a semiclassical system that represents the interaction between matter and a given field. The concept of Fisher Information measure ($\mathcal{F}$) on using as a quantifier of the process, we find that it adequately describes the transition, detecting the most salient details of the changeover. Used in conjunction with other possible information quantifiers, such as the Normalized Shannon Entropy ($\mathcal{H}$) and the Statistical Complexity ($\mathcal{C}$) by recourse to appropriate planar representations like the Fisher Entropy ($\mathcal{F} \times \mathcal{H}$) and Fisher Complexity ($\mathcal{F} \times \mathcal{C}$) planes, one obtains a better visualization of the transition than that provided by just one quantifier by itself. In the evaluation of these Information Theory quantifiers, we used the Bandt and Pompe methodology for the obtention of the corresponding probability distribution.

1. Introduction

Since the introduction of the decoherence concept in the early 1980s, by, among others, Zeh and Zurek [1–3], the emergence of the classical world from its quantal substratum mechanics has become a subject of much interesting work an intense discussion. In this work we will embark on such a discussion by revisiting the classical limits of a special five-dimensional model that represents a matter–field interaction and whose dynamics, that has received exhaustive attention in the past years, describes a bona fide quantum–classical transition (QCT). This QCT can be, interestingly enough, visualized by recourse to a special model's parameter, whose numerical evolution between the value one and infinity makes the model to represent a strictly quantum system at first, then a semi-quantum one, and eventually a purely classical one. The pertinent stages of such evolution are well known.

What do we intend to do then? Our goal is to tackle the description of these stages not with dynamical tools (this has been already abundantly done) but with statistical and information theoretic ones pertaining to the field of nonlinear time-series analysis, which will hopefully yield novel insights into the associated physics. In this sense, an important step was effected in Ref. [4] that revolves around the utilization of Shannon's entropy. Here we will show that the conjunction of several information quantifiers significantly improves the descriptive power of the information theory approach and does yield interesting physics insights.

* Corresponding author at: Departamento de Física, Instituto de Ciências Exatas, Universidade Federal de Minas Gerais, Av. Antônio Carlos, 6627 - Campus Pampulha, 31270-901 Belo Horizonte - MG, Brazil.

E-mail addresses: kowalski@fisica.unlp.edu.ar (A.M. Kowalski), mtmartin@fisica.unlp.edu.ar (M.T. Martín), plastino@fisica.unlp.edu.ar (A. Plastino), oarosso@fibertel.com.ar, oarosso@gmail.com (O.A. Rosso).

0378-4371/$ – see front matter
doi:10.1016/j.physa.2011.02.009

2. The classical limit of quantum mechanics (a special semiclassical model)

It is clear that much quantum insight is to be gained from semiclassical perspectives. Several methodologies are available (WKB, Born–Oppenheimer approach, etc.). The models of Refs. [5–7], consider two interacting systems: one of them classical, the other quantal. This makes sense whenever the quantum effects of one of the two systems are negligible in comparison to those of the other one. Examples include Bloch equations, two-level systems interacting with an electromagnetic field within a cavity, collective nuclear motion, etc. We will here deal with a special bipartite system that represents the zero mode contribution of a strong external field to the production of charged meson pairs [6,7], whose Hamiltonian reads

$$\hat{H} = \frac{1}{2}\left(\frac{\hat{p}^2}{m_q} + \frac{{P_A}^2}{m_{\rm cl}} + m_q\omega^2\hat{x}^2\right), \tag{1}$$

where (i) $\hat{x}$ and $\hat{p}$ are quantum operators, (ii) A and P_A classical canonical conjugate variables and (iii) $\omega^2 = {\omega_q}^2 + e^2A^2$ is an interaction term that introduces nonlinearity, ω_q being a frequency. The quantities m_q and $m_{\rm cl}$ are masses corresponding to the quantum and classical systems, respectively. As shown in Ref. [7], in dealing with Eq. (1) one faces an autonomous system of nonlinear coupled equations

$$\begin{aligned}
&\frac{{\rm d}\langle\hat{x}^2\rangle}{{\rm d}t} = \frac{\langle\hat{L}\rangle}{m_q},\\
&\frac{{\rm d}\langle\hat{p}^2\rangle}{{\rm d}t} = -m_q\,\omega^2\langle\hat{L}\rangle,\\
&\frac{{\rm d}\langle\hat{L}\rangle}{{\rm d}t} = 2\left(\frac{\langle\hat{p}^2\rangle}{m_q} - m_q\,\omega^2\langle\hat{x}^2\rangle\right),\\
&\frac{{\rm d}A}{{\rm d}t} = \frac{P_A}{m_{\rm cl}},\\
&\frac{{\rm d}P_A}{{\rm d}t} = -e^2 m_q\,A\langle\hat{x}^2\rangle
\end{aligned} \tag{2}$$

where $\hat{L} = \hat{x}\hat{p} + \hat{p}\hat{x}$. The system of Eq. (2), follows immediately from Ehrenfest's relations [8]. Here (1) is of semiclassical nature. Were it of purely quantal one, Eq. (2) would cease to be a closed system.

To study the classical limit we also need to consider the classical counterpart of the Hamiltonian given by Eq. (1)

$$H = \frac{1}{2}\left(\frac{p^2}{m_q} + \frac{{P_A}^2}{m_{\rm cl}} + m_q\omega^2x^2\right), \tag{3}$$

where all the variables are classical. Recourse to Hamilton's equations allows one to find the classical version of Eq. (2). These equations are identical in form to Eq. (2) after suitable replacement of quantum mean values by classical variables, i.e., $\langle\hat{x}^2\rangle \Rightarrow x^2$, $\langle\hat{p}^2\rangle \Rightarrow p^2$ and $\langle\hat{L}\rangle \Rightarrow L = 2xp$. The classical limit is obtained by letting the "relative energy"

$$E_r = \frac{E}{I^{1/2}\omega_q} \to \infty, \tag{4}$$

($E_r \geq 1$), where E is the total energy of the system and I is an invariant of the motion described by the system of equations previously introduced (Eq. (2)), related to the Uncertainty Principle

$$I = \langle\hat{x}^2\rangle\langle\hat{p}^2\rangle - \frac{\langle\hat{L}\rangle^2}{4} \geq \frac{\hbar^2}{4}. \tag{5}$$

A classical computation of I yields $I = x^2p^2 - L^2/4 \equiv 0$. Thus, I vanishes when it is evaluated using the classical variables A and P_A, for all t, i.e. $I(A, P_A) = 0$, a fact that exhibits the self-consistency of our methodology. E_r is of course a relative energy. It compares the actual one with the pseudo-energy $E_I = I^{1/2}\omega_q$, related to the Uncertainty Principle. For $E \gg E_I$ the classical limit obtains.

A measure of the degree of convergence between classical and quantum results in the limit of Eq. (4) is given by the norm $\mathcal{N}$ of the vector $\Delta u = u - u_{\rm cl}$ [8],

$$\mathcal{N}_{\Delta u} = |u - u_{\rm cl}|, \tag{6}$$

where the three components vector $u = (\langle\hat{x}^2\rangle, \langle\hat{p}^2\rangle, \langle\hat{L}\rangle)$ is the "quantum" part of the solution of the system defined by Eq. (2) and $u_{\rm cl} = (x^2, p^2, L)$ its classical counterpart.

A detailed study of this model was performed in Ref. [7]. The main results of this reference, pertinent for our discussion, can be succinctly detailed as follows: in plotting diverse dynamical quantities as a function of E_r (as it grows from unity to ∞), one finds *an abrupt change in the system's dynamics for a special value of* E_r, *to be denoted by* ${E_r}^{\rm cl} = 21.55264$. From this

value onwards, the pertinent dynamics starts converging to the classical one. It is thus possible to assert that ${E_r}^{\rm cl}$ provides us with an *indicator* of the presence of a quantum–classical "border". The zone $E_r < {E_r}^{\rm cl}$, corresponds to the semi-quantal regime [7]. This regime, in turn, is characterized by *two* different sub-zones. One of them is an almost purely quantal one, in which the microscopic quantal oscillator is just slightly perturbed by the classical one, and the other section exhibits a transitional nature (semi-quantal). The border between these two sub-zones can be well characterized by a relative energy value ${E_r}^{\mathcal{P}} = 3.3282$. A significant feature of this point resides in the fact that, for $E_r \geq {E_r}^{\mathcal{P}}$, *chaos is always found*. The relative number of chaotic orbits (with respect to the total number of orbits) grows with E_r and tends to unity for $E_r \to \infty$ [7].

Thus, as E_r grows from $E_r = 1$ (the "pure quantum instance") to $E_r \to \infty$ (the classical situation), a significant series of *morphology changes* is detected, specially in the transition zone (${E_r}^{\mathcal{P}} \leq E_r \leq {E_r}^{\rm cl}$). The concomitant orbits exhibit features that are not easily describable in terms of Eq. (6), which is a *global* measure of the degree of convergence in amplitude (of the signal). What one needs instead is *a statistical type of characterization*, involving simultaneously the notions of entropy, statistical complexity [4,9,10], and Fisher Information.

3. Information quantifiers

3.1. Fisher information measure and Shannon entropy

Given a continuous probability distribution function (PDF) $f(x)$, its *Shannon Entropy* S is Ref. [11]

$$S[f] = -\int f \ln(f)\, {\rm d}x, \tag{7}$$

a measure of "global character" that it is not too sensitive to strong changes in the distribution taking place on a small-sized region.

Such is not the case with *Fisher's Information Measure (FIM)* $\mathcal{F}$ [12,13], which constitutes a measure of the gradient content of the distribution f, thus being quite sensitive even to tiny localized perturbations. It reads [12]

$$\mathcal{F}[f] = \int \frac{|\vec{\nabla} f|^2}{f}\, {\rm d}x. \tag{8}$$

FIM can be variously interpreted as a measure of the ability to estimate a parameter, as the amount of information that can be extracted from a set of measurements, and also as a measure of the state of disorder of a system or phenomenon [12,14]. Its most important property is the so-called Cramer–Rao bound, that we recapitulate in one-dimension, for the sake of simplicity. The classical Fisher information associated with translations of a one-dimensional observable x with corresponding probability density $f(x)$ is Ref. [15]

$$I_x = \int {\rm d}x f(x) \left(\frac{\partial \ln f(x)}{\partial x}\right)^2, \tag{9}$$

which obeys the above referred to the Cramer–Rao inequality

$$(\Delta x)^2 \geq I_x^{-1} \tag{10}$$

involving the variance of the stochastic variable x [15]

$$(\Delta x)^2 = \langle x^2 \rangle - \langle x \rangle^2 = \int {\rm d}x f(x)\, x^2 - \left(\int {\rm d}x f(x)\, x\right)^2. \tag{11}$$

We insist in remarking that the gradient operator significantly influences the contribution of minute local f-variations to FIM's value, so that the quantifier is called a "local" one. Note that Shannon's entropy decreases with skewed distribution, while Fisher's information increases in such a case. Local sensitivity is useful in scenarios whose description necessitates appeal to a notion of "order" (see below).

Now let $P = \{p_i;\ i = 1, \ldots, N\}$ be a discrete probability distribution set, with N the number of possible states of the system under study. The concomitant problem of loss of information due to the discretization has been thoroughly studied (see, for instance, [16–18] and the references therein) and, in particular, it entails the loss of FIM's shift-invariance, which is of no importance for our present purposes. In the discrete case, Shannon's quantifier is evaluated via

$$S[P] = -\sum_{i=1}^{N} p_i\, \ln(p_i), \tag{12}$$

and we define a "normalized" Shannon entropy as $\mathcal{H}[P] = S[P]/S_{\rm max}$, where the denominator obtains for a uniform probability distribution.

For the FIM-computation Measure we follow the proposal of Ferri and coworkers [19] (among others)

$$\mathcal{F}[P] = \frac{1}{4}\sum_{i=1}^{N-1} 2\frac{(p_{i+1}-p_i)^2}{(p_{i+1}+p_i)}\,. \tag{13}$$

If our system is in a very ordered state and thus is represented by a very narrow PDF, we have a Shannon Entropy $S \sim 0$ and a Fisher's Information Measure $\mathcal{F} \sim F_{\max}$. On the other hand, when the system under study lies in a very disordered state one gets an almost flat PDF and $S \sim S_{\max}$ while $\mathcal{F} \sim 0$. Of course, $S_{\max}$ and $F_{\max}$ are, respectively, the maximum possible values for Shannon's Entropy and Fisher's Information Measure. One can state that the general behavior of the Fisher Information Measure is opposite to that of the Shannon Entropy [20].

3.2. Statistical complexity

The complexity degree of dynamical systems has no universal definition, however statistical complexity can be understood as a measure that captures not only the system's randomness but also considers its physical components (structural correlations) [21]. In this work, we use a particular form of statistical complexity measure that is cast as the product of the normalized Shannon Entropy and the normalized Jensen–Shannon divergence. We call it the MPR-Statistical Complexity [22], a variant of the measure originally introduced in the pioneer reference [23]. An important property of this measure is that it presents "zero" value for the extreme cases given by complete order and total random behavior.

The MPR-Statistical Complexity is defined by

$$\mathcal{C}[P] = \mathcal{Q}[P, P_e]\cdot\mathcal{H}[P], \tag{14}$$

where, to the probability distribution P, we associate the normalized entropic measure $\mathcal{H}[P] = S[P]/S_{\max}$, with $S_{\max} = S[P_e]$ ($0 \leq H_S \leq 1$). We take here the disequilibrium $\mathcal{Q}$ to be defined in terms of the extensive Jensen divergence [24] according to

$$\mathcal{Q}[P, P_e] = Q_0\{S[(P+P_e)/2] - S[P]/2 - S[P_e]/2\}. \tag{15}$$

with

$$Q_0 = -2\left\{\left(\frac{N+1}{N}\right)\ln(N+1) - 2\ln(2N) + \ln N\right\}^{-1}, \tag{16}$$

a normalization constant that makes $0 \leq \mathcal{Q} \leq 1$. This SCM-version [24,25] is (i) able to grasp essential details of the dynamics, (ii) an intensive quantity, and (iii) capable of discerning among different degrees of periodicity and chaos.

3.3. Probability distribution function and Bandt–Pompe approach

An important issue for the evaluation of the information quantifiers is the proper determination of the underlying probability distribution function P, associated to a given dynamical system or time series. Many schemes have been proposed for a proper selection of it. We can mention, among others: (a) frequency count [26] (b) procedures based on amplitude statistics (histograms) [27], (c) binary symbolic dynamics [28], (d) Fourier analysis [29], and (e) wavelet transform [30,31]. Their applicability depends on particular characteristics of the data. In all these cases the global aspects of the dynamics can be somehow captured, but the different approaches are not equivalent in their ability to discern all the relevant physical details. One must also acknowledge the fact that the above techniques are introduced in a *rather ad hoc fashion and are not directly derived from dynamical properties of the system under study*,. This can be adequately effected, for instance, by recourse to the Bandt–Pompe ordinal-patterns methodology [32].

The symbolic methodology proposed by Bandt and Pompe is based on the details of the series time delay reconstruction procedure (the ordinal patterns present in the time series). Here, causal, dynamic information should be expected to help getting better results. The probability distribution P is obtained once we fix the embedding dimension D and the time delay τ [32]. Furthermore, the ordinal pattern probability distribution is invariant with respect to nonlinear monotonous transformations. Thus, nonlinear drifts or scalings artificially introduced by a measurement device do not modify the quantifier estimations, a relevant property for the analysis of experimental data. These are the main advantages with respect to more conventional methods based on range partitioning.

We used this methodology here (for details of the Bandt–Pompe methodology, see [25,33]). The probability distribution P is obtained once we fix the embedding dimension D and the embedding delay τ. The former parameter plays an important role for the evaluation of the appropriate probability distribution, since D determines the number of accessible states, given by $D!$. Moreover, it was established that the length N of the time series must satisfy the condition $N \gg D!$ in order to achieve a proper differentiation between stochastic and deterministic dynamics [22]. In particular, Bandt and Pompe [32] suggest for practical purposes to work with $3 \leq D \leq 7$. With respect to the selection of the other parameter, Bandt and Pompe specifically considered an embedding delay $\tau = 1$ in their foundational paper [32]. In the present work the value $D = 5$ was selected, since we deal time series of at least $N = 5000$ data-points, the condition $N \gg D!$ is clearly satisfied. We take the customary time delay $\tau = 1$ [32].

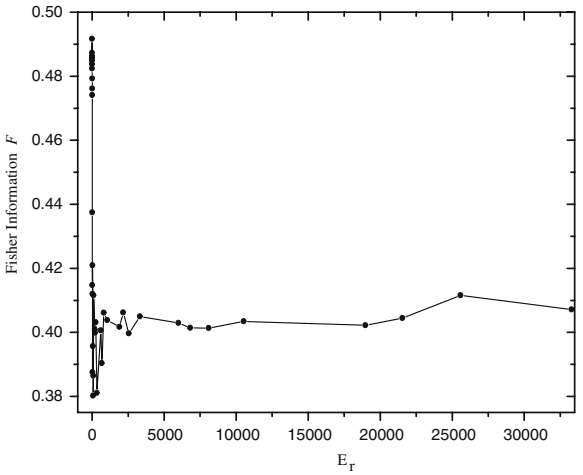

Fig. 1. Fisher Information $\mathcal{F}$ vs. E_r for a broad E_r range. See the desired convergence to classicality.

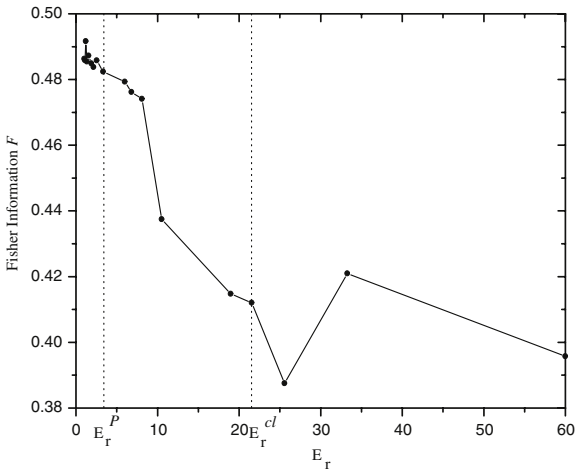

Fig. 2. Fisher Information $\mathcal{F}$ vs. E_r for a range for which the regions of the process can be clearly appreciated. Fisher's information distinguishes and correctly describes our three zones: quantal, transition, and classical. They are delimited by special E_r values, namely, $E_r{}^{\mathcal{P}} = 3.3282$ and $E_r{}^{\mathrm{cl}} = 21, 55264$.

4. Results and discussion

Our data-points emerge as the solutions of Eq. (2), from which we extract the values of $\langle x^2\rangle$ and the (classical) values of x^2 at the time t (for a fixed E_r). We have also performed these calculations replacing the above values for those corresponding to $\langle p^2\rangle - p^2$ together with $\langle L\rangle - L$. The replacements lead to entirely similar final results. We pass now to a description of them.

In obtaining our numerical results we chose $m_q = m_{\mathrm{cl}} = \omega_q = e = 1$ for the system's parameters. For the initial conditions needed to tackle our system (Eq. (2)) we fixed E and then varied I so as to obtain our different E_r-values. Additionally, we set $\langle L\rangle(0) = L(0) = 0, A(0) = 0$ (both in the quantum and the classical instances).

Classical curves are generated varying $x^2(0)$ within the interval $(0, 2E)$. Quantal ones for each I-value (and associated E_r), varying $\langle x^2\rangle(0)$ within the interval $(E - \sqrt{E^2 - I}, E + \sqrt{E^2 - I})$ with $I \leq E^2$. We have considered curves contain up to 50000 points for each $[x^2(0), \langle x^2\rangle(0)]$ pair.

Figs. 1–3 depict results corresponding to $E = 0.6$ and $\langle x^2\rangle(0)$ in the interval $x^2(0) < \langle x^2\rangle(0) \leq 0.502$, with $x^2(0) = 0.012$. We consider 5000 data-points per initial condition and take 41 different values of I. Particular care has been devoted to the curves here displayed, because they have also been studied using different tools, namely, entropy and statistical complexity, evaluated by employing either the wavelet approach or the Bandt and Pompe method with different probability space metrics [4,9,10]. The conceptual characteristics of the results are independent of the initial conditions and of the number of points employed to construct our time series.

Fig. 1 depicts the Fisher Information $\mathcal{F}$ vs. E_r for a large range of the latter's variation. Fig. 2 amplifies things in a range long enough that allows one to visualize the three zones of the transition process. We find, as a first result, that $\mathcal{F}$ evaluated

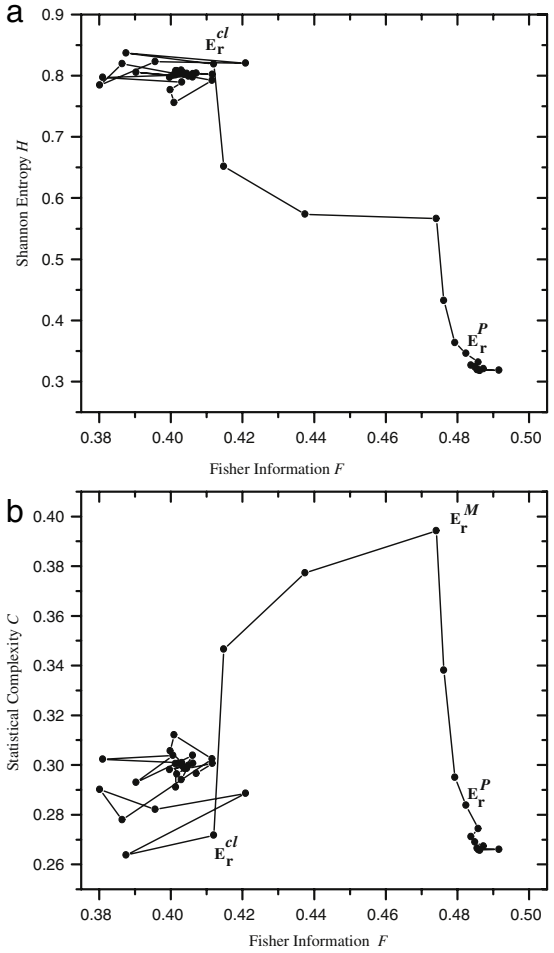

Fig. 3. Plot of the (a) $\mathcal{F} \times \mathcal{H}$-plane and (b) the $\mathcal{F} \times \mathcal{C}$-plane. The three relevant regions are visible. Figure (b) exhibits a third relevant E_r point, called E_r^M, where maximum complexity is attained. This E_r-value divides approximately into two sections the transitional region, namely, one in which the quantum–classical mixture characterizes a phase–space with more non-chaotic than chaotic curves and other for which this feature is reversed.

according to Eq. (13), correctly *distinguishes* indeed the three well-known physical sections of our process, i.e., quantal, transitional, and classic region, as delimited by, respectively, ${E_r}^{\mathcal{P}}$ and ${E_r}^{\mathrm{cl}}$. Notice please the abrupt change in the slope of the curve of Fig. 2 taking place at ${E_r}^{\mathcal{P}}$. The transition zone is clearly demarcated between that point and ${E_r}^{\mathrm{cl}}$. From there on $\mathcal{F}$ tends to its classical value at the same time as the quantum solutions of Eq. (2) begin to converge towards their classical counterparts (Fig. 1). As a second result we notice that Fisher's information measure (FIM) aptly describes our three zones (see Fig. 2). FIM is maximal in the quantum region, characterized by quasi-periodic solutions of Eq. (2), and a minimum in the classic sector, where the dynamics is chaotic. Intermediate FIM-values are found in the transitional zone, where periodicity and chaos coexist.

Fig. 3(a) displays the so-called Fisher–Shannon $\mathcal{F} \times \mathcal{H}$-plane while Fig. 3(b) does so for a different plane, the Fisher Complexity $\mathcal{F} \times \mathcal{C}$-one The reader is referred to similar (but different) representations, corresponding to (i) $\mathcal{H}$ and (ii) $\mathcal{C}$ vs. E_r in Ref. [4]. Classical and quantum regions occupy the right-hand and the left-hand side of the graphs, respectively. The transition region corresponds to an intermediate planar location. According to Fig. 3(a), classicality is associated to high entropy and low FIM, a situation that reverses itself in the quantum region. The transition zone becomes clearly delimited between points ${E_r}^{\mathrm{cl}}$ and ${E_r}^{\mathcal{P}}$. In turn, according to Fig. 3(b) both classicality and the quantum domain are associated to low complexity. $\mathcal{C}$ is instead high in the transitional region. We will return in the Conclusions to this point.

Continuing with Fig. 3(b), we see that the transition zone is again clearly visible between points ${E_r}^{\mathrm{cl}}$ and ${E_r}^{\mathcal{P}}$. A third relevant E_r-value is noticeable in Fig. 3(b), namely, the one at which an absolute maximum of $\mathcal{C}$ is found, at $E_r^M = 8,0904$. There, great instabilities in the system's dynamics ensue, as the solutions of Eq. (2) [7] experience a complex process. Indeed, E_r^M divides into two sections the transitional region: (i) one in which the quantum–classical mixture characterizes a phase–space with more non-chaotic than chaotic curves and (ii) other, in which this feature is reversed [7]. Note in Fig. 3(b) that from E_r^M-eastwards a significant slope change.

5. Conclusions

In the present work we have studied the classical–quantal frontier problem by using the Fisher Information. We dealt with the dynamics generated by a semiclassical Hamiltonian that represents the zero mode contribution of a strong external field to the production of charged meson pairs [6,7].

The highlights of the road towards classicality are described by recourse to the relative energy E_r given by Eq. (4). As E_r grows from $E_r = 1$ (the "pure quantum instance") to $E_r \to \infty$ (the classical situation), a significant series of *morphology changes* is detected for the solutions of the system of nonlinear coupled equations Eq. (2) [7]. The concomitant process takes place in three stages: quantal, transitional, and classic, delimited, respectively, by special values of E_r, namely, ${E_r}^{\mathcal{P}}$ and ${E_r}^{\mathrm{cl}}$.

We find, as first result, that the Fisher Information $\mathcal{F}$ correctly distinguishes the three well-known physical zones or sections of our process, i.e., quantal, transitional, and classic, as delimited by, respectively, ${E_r}^{\mathcal{P}}$ and ${E_r}^{\mathrm{cl}}$. Second, FIM correctly describes the three process regions, taking maximal values in the quantum region characterized by quasi-periodic dynamics and minimal ones for classicality, that has associated to it chaotic dynamics. FIM takes intermediate values in the transition sector, where quasi-periodicity coexists with chaos. The two planar representations here studied, namely, $\mathcal{F} \times \mathcal{H}$-plane and $\mathcal{F} \times \mathcal{C}$-one (Fig. 3) allows one to easily visualize the physics-associated E_r-evolution, making it plain the existence of three different zones.

Finally, our results seem to indicate that wherever the underlying dynamics is known to obey well-established rules (classical or quantum ones), the complexity quantifier adopts low values. However, if the underlying behavior rules are not clear (or unknown), a high complexity becomes the signature of such state of affairs.

Acknowledgements

A.M. Kowalski is supported by CIC of Argentina. O.A. Rosso acknowledges partial support from CONICET, Argentina, and CAPES, PVE fellowship, Brazil.

References

[1] H.D. Zeh, Why Bohm's quantum theory? Found. Phys. Lett. 12 (1999) 197–200.
[2] W.H. Zurek, Pointer basis of quantum apparatus: into what mixture does the solutions of (2) wave packet collapse? Phys. Rev. D 24 (1981) 1516–1525.
[3] W.H. Zurek, Decoherence, einselection, and the quantum origins of the classical, Rev. Modern Phys. 75 (2003) 715–775.
[4] A.M. Kowalski, M.T. Martín, A. Plastino, O.A. Rosso, Bandt–Pompe approach to the classical-quantum transition, Physica D 233 (2007) 21–31.
[5] L.L. Bonilla, F. Guinea, Collapse of the wave packet and chaos in a model with classical and quantum degrees of freedom, Phys. Rev. A 45 (1992) 7718–7728.
[6] F. Cooper, J. Dawson, S. Habib, R.D. Ryne, Chaos in time-dependent variational approximations to quantum dynamics, Phys. Rev. E 57 (1998) 1489–1498.
[7] A.M. Kowalski, A. Plastino, A.N. Proto, Classical limits, Phys. Lett. A 297 (2002) 162–172.
[8] A.M. Kowalski, M.T. Martín, J. Nuñez, A. Plastino, A.N. Proto, Quantitative indicator for semiquantum chaos, Phys. Rev. A 58 (1998) 2596–2599.
[9] A.M. Kowalski, M.T. Martín, A. Plastino, A. Proto, O.A. Rosso, Wavelet statistical complexity analysis of classical limit, Phys. Lett. A 311 (2003) 180–191.
[10] A.M. Kowalski, M.T. Martín, A. Plastino, O.A. Rosso, Entropic non-triviality, the classical limit, and geometry-dynamics correlations, Internat. J. Modern Phys. B 14 (2005) 2273–2285.
[11] C. Shannon, W. Weaver, The Mathematical Theory of Communication, University of Illinois Press, Champaign, IL, 1949.
[12] B.R. Frieden, Science from Fisher Information: A Unification, Cambridge University Press, Cambridge, 2004.
[13] R.A. Fisher, On the mathematical foundations of theoretical statistics, Philos. Trans. R. Soc. Lond. Ser. A 222 (1922) 309–368.
[14] A.L. Mayer, C.W. Pawlowski, H. Cabezas, Fisher Information and dinamic regime changes in ecological systems, Ecol. Model. 195 (2006) 72–82.
[15] M.J.W. Hall, Quantum properties of classical Fisher information, Phys. Rev. A 62 (2000) 012107.
[16] K. Zografos, K. Ferentinos, T. Papaioannou, Discrete approximations to the Csiszár, Renyi, and Fisher measures of information, Canad. J. Statist. 14 (1986) 355.
[17] L. Pardo, D. Morales, K. Ferentinos, K. Zografos, Discretization problems on generalized entropues and *R*-divergences, Kybernetika 30 (1994) 445–460.
[18] M. Madiman, O. Johnson, I. Kontoyiannis, Fisher information, compound Poisson approximation, and the Poisson channel, in: IEEE Int. Symp. Inform. Th., Nice, June 2007.
[19] G.I. Ferri, F. Pennini, A. Plastino, LMC-complexity and various chaotic regimes, Phys. Lett. A 373 (2009) 2210–2214.
[20] F. Pennini, A. Plastino, Reciprocity relations between ordinary temperature and the Frieden–Soffer Fisher temperature, Phys. Rev. E 71 (2005) 047102.
[21] J.P. Crutchfield, K. Young, Inferring statistical complexity, Phys. Rev. Lett. 63 (1989) 105–108.
[22] O.A. Rosso, H.A. Larrondo, M.T. Martín, A. Plastino, M.A. Fuentes, Distinguishing Noise from chaos, Phys. Rev. Lett. 99 (2007) 154102.
[23] R. López-Ruiz, H. Mancini, X. Calbet, A statistical measure of complexity, Phys. Lett. A 209 (1995) 321–326.
[24] P.W. Lamberti, M.T. Martín, A. Plastino, O.A. Rosso, Entropic nontriviality measure, Physica A 334 (2004) 119–131.
[25] O.A. Rosso, L. De Micco, H.A. Larrondo, M.T. Martín, A. Plastino, Generalized statistical complexity measure, Internat. J. Bifur. Chaos 20 (2010) 775–785.
[26] O.A. Rosso, H. Craig, P. Moscato, Shakespeare and other english renaissance authors as characterized by information theory complexity quantifiers, Physica A 388 (2009) 916–926.
[27] L. De Micco, C.M. Gonzalez, H.A. Larrondo, M.T. Martín, A. Plastino, O.A. Rosso, Randomizing nonlinear maps via symbolic dynamics, Physica A 387 (2008) 3373–3383.
[28] K. Mischaikow, M. Mrozek, J. Reiss, A. Szymczak, Construction of symbolic dynamics from experimental time series, Phys. Rev. Lett. 82 (1999) 1114–1147.
[29] G.E. Powell, I.C. Percival, A spectral entropy method for distinguishing regular and irregular motion of Hamiltonian systems, J. Phys. A: Math. Gen. 12 (1979) 2053–2071.
[30] O.A. Rosso, S. Blanco, J. Jordanova, V. Kolev, A. Figliola, M. Schürmann, E. Başar, Wavelet entropy: a new tool for analysis of short duration brain electrical signals, J. Neurosci. Methods 105 (2001) 65–75.
[31] O.A. Rosso, L. Mairal, Characterization of time dynamical evolution of electroencephalographic records, Physica A 312 (2002) 469–504.
[32] C. Bandt, B. Pompe, Permutation entropy: a natural complexity measure for time series, Phys. Rev. Lett. 88 (2002) 174102.
[33] O.A. Rosso, L. De Micco, A. Plastino, H.A. Larrondo, Info-quantifiers' map-characterization revisited, Physica A 389 (2010) 4604–4612.